UCRL-JC-123983
PREPRINT
CONF-9506148--2

Impurity Effects on Bonding Charge in Ni_3Al

Sheng N. Sun
Nicholas Kioussis
Say-Peng Lim
A. Gonis
W. H. Gourdin

This paper was prepared for submittal to the
NATO Advanced Study Institute on Stability of Materials
Corfu, Greece, June 25-July 7, 1995

May 14, 1996

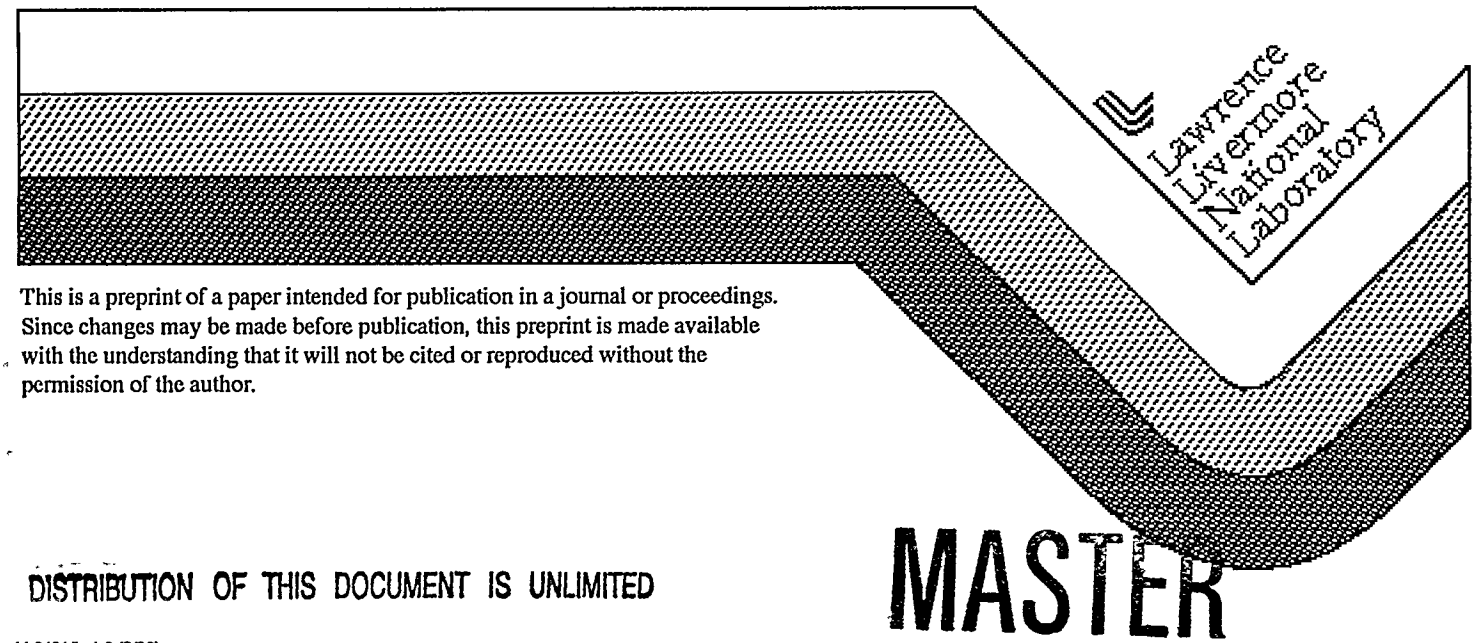

IMPURITY EFFECTS ON BONDING CHARGE IN Ni_3Al

Sheng N. Sun, Nicholas Kioussis, and Say-Peng Lim

Department of Physics and Astronomy
California State University, Northridge, CA 91330

A. Gonis and W. Gourdin

Lawrence Livermore National Laboratory,
Department of Chemistry and Material Science
Livermore, CA 94550

INTRODUCTION

Microalloying studies have shown[1] that doping with certain impurities, which prefer to segregate towards grain boundaries, can significantly improve the ductility of polycrystalline Ni_3Al.[2] The addition of only 0.05 wt% (0.25 at%) of boron increases the room temperature elongation of polycrystalline Ni_3Al from a few percent to values of 45-50%. This effect, however, is only observed in specimens that contain excess Ni. Because boron is known to segregate preferentially to grain boundaries, one explanation for its dramatic effect on ductility is that it promotes better cohesion across the grain boundary planes.[3] More recent experiments have shown that boron also improves the ductility of single Ni_3Al crystals,[4] suggesting that a "bulk effect" should be considered in addition to the grain boundary strengthening effect of boron when explaining the improvement in ductility of polycrystalline Ni_3Al due to B additions.

While the *intrinsic* factors, such as poor grain boundary cohesion, are important, in many cases dominant, in limiting ductility, recent work by George *et al* has shown[5] that *extrinsic* factors, in particular the humidity, can be a major cause of low ductility in some systems. Their results demonstrate that the poor ductility commonly observed in air tests involves the dissociation of H_2O to generate atomic hydrogen, which diffuses into the region of the crack tip and promotes brittle crack propagation. George *et al* [5] have suggested that the principal role of boron in ductlizing Ni_3Al is to suppress the environmental embrittlement.

The purpose of the this work is to understand the electronic mechanism underlying the contrasting effects of the boron-induced strengthening and the hydrogen-induced embrittlement in Ni_3Al. To this end, we have carried out full potential linear-muffin-tin-orbital total energy calculations to investigate the effects of boron and hydrogen in Ni_3Al, and to study the changes of bonding associated with these impurities.

Figure 1. Supercell geometry used in the calculation. The filled, empty, and gray shaded circles represent Ni, Al, and X atom, respectively (X stands for the Boron or Hydrogen impurity). The two types of octahedral sites for the impurity. are denoted by X(7) and X(8), respectively.

COMPUTATIONAL METHOD

Our method of solving the electronic structure problem is based on the full-potential linear-muffin-tin-orbital (FLMTO) method, and has been described in detail elsewhere.[6] In treating intermetallic systems, the full potential approach is essential because of the large charge anisotropy of these systems. The supercell employed in our calculations is shown in Fig. 1. Inequivalent atoms in the cell are denoted by numerical labels (enclosed in parenthesis), depending on their point group symmetry. Based on X-ray diffraction intensity ratios, Masahashi *et al.*[7] conclude that boron occupies octahedral interstices in the Ni_3Al structure. Therefore, in order to study the effect of the local environment of the impurity on the electronic structure, the impurity (labeled by X) was placed at two different octahedral interstitial sites: 1) At the center of the octahedral cell [X(7)] and 2) at the center of the cube edge [X(8)]. We will refer to the X(7) and X(8) sites as Ni-rich and Ni-deficient octahedral-sites (O-sites), respectively. Such an arrangement corresponds to an impurity concentration of 7.7 at.% when one of the octahedral sites is occupied. In all calculations, atomic relaxation was ignored and the lattice constant was kept frozen at the value of 3.568$\AA$ for pure Ni_3Al.[8] The muffin-tin radii of 1.07$\AA$ were chosen to be equal for both Ni and Al atoms. The muffin-tin radii for the boron and hydrogen impurity were chosen also to be equal at 0.71$\AA$.

NUMERICAL RESULTS AND DISCUSSION

First we present the bonding charge density, $\Delta\rho(\mathrm{r}) = \rho_{solid}(\mathrm{r}) - \sum_\alpha \rho_\alpha(\mathrm{r}-\mathrm{r}_\alpha)$, where $\rho_{solid}(\mathrm{r})$ is the self-consistent charge density for the solid, $\rho_\alpha(\mathrm{r})$ is the atomic charge

Figure 2. The charge density difference between Ni_3Al and the superposition of neutral Ni and Al atomic charge densities on the (110) planes. The solid (dotted) contours denote contours of increased (decreased) density as atoms are brought together to form the Ni_3Al crystal. Contours start from $\pm 8.0 \times 10^{-4}$ e/(a.u.)^3 and increase successively by a factor of $\sqrt{2}$.

density, and r_α is the position of the atom, on the (110) plane in Fig. 2 in units of 10^{-3} e/(a.u.)^3. Here, solid and dotted curves represent contours of increased (accumulation) and decreased (depletion) electronic charge density. We find that the depletion of electron density at the aluminum sites is accompanied by significant *anisotropic* build-up of the directional d-bonding charge at the nickel sites. The bonding charge accumulation at the Ni site is along the nearest-neighbor (NN) Ni-Al and next-nearest-neighbor (NN) Ni-Ni directions. The bonding directionality is mainly caused by the polarization of p-electrons at the Al sites as a result of the p-d hybridization effect. One can also see a significant build-up of the interstitial bonding charge at the octahedral sites [sites between next-nearest-neighbor (NNN) Ni atoms and NNN Al atoms] between the (001) Ni-Al planes. These results are in qualitative agreement with those of recent warped-muffin-tin LMTO electronic structure calculations.[9] However, it is *the non-spherical corrections* to the spherical potential that yield the directionality of the d-bonding charge at the Ni sites. Thus, the bonding mechanism in Ni_3Al involves the combination of charge transfer and strong Al-p/Ni-d hybridization effects.

In order to study the effect of the local environment of the impurity on the electronic structure, we consider two different types of octahedral sites X(7) and X(8) in Fig. 1. To compare the energetics of the different impurity configurations we have calculated the impurity formation energy, $\Delta E_{imp} = E_{tot}(Ni_3AlX) - E_{tot}(Ni_3Al) - E_{tot}(X)$. Here, $E_{tot}(Ni_3AlX)$ is the total energy of the supercell with the impurity X placed at a certain octahedral site, $E_{tot}(Ni_3Al)$ is the total energy of the supercell without the impurity and $E_{tot}(X)$ is the total energy of an isolated impurity atom. We find that the impurity formation energies for a boron impurity placed at the Ni-rich [X(7)] and Ni-deficient [X(8)] octahedral sites in Ni_3Al, are -4.4 eV/(unit cell) and -0.08 eV/(unit cell),

Figure 3. Boron-induced charge density of $Ni_3AlB_{\frac{1}{3}}$. Boron occupies the Ni-rich octahedral site [X(7)]. Solid (dotted) contours denote positive (negative) induced charge density. Contours start from $\pm 8.0 \times 10^{-4}$ e/(a.u.)^3 and increase successively by $\sqrt{2}$, (a) on the (110) plane and (b) on the (002) plane.

respectively. Thus, boron prefers to occupy octahedral sites which are surrounded by nearest-neighbor Ni atoms.

To understand the effect of absorbed boron on the bonding properties of Ni_3Al we next consider the redistribution of charge induced by the impurity atom when placed at the Ni-rich octahedral site [X(7)]. This can be best described by the *difference of bonding charge density* between Ni_3AlB and Ni_3Al, i.e., $\Delta\rho_{ind}(r) = \Delta\rho_{solid}(Ni_3AlX) - \Delta\rho_{solid}(Ni_3Al) = \rho_{solid}(Ni_3AlX) - \rho_{solid}(Ni_3Al) - \rho_{atom}(X)$. We will refer to $\Delta\rho_{ind}(r)$ as the impurity-induced charge density. The impurity-induced charge density on the (110) and (002) planes is shown in Figs. 3(a) and 3(b), respectively. One can see that the enhancement of bonding charge around the Ni(4) site in Fig. 3(a) is quite asymmetric relative to the (001) plane through the atom. This is expected because the presence of boron breaks such a mirror symmetry. Though boron induces a decrease of the total MT valence charge in the Ni(3) site, the redistribution of the bonding charge about the Ni(3) site is significant. A comparison of Figs. 2 and 3(a) shows that boron induces a charge accumulation about Ni(3) in a direction where there is a depletion of the bonding charge $\Delta\rho(r)$ in the pure Ni_3Al system. Thus, the bonding-charge directionality of Ni(3) is *reduced* due to the presence of a small percentage of boron. More importantly, boron causes a significant build-up of interstitial charge near the (001) planes containing solely Ni atoms [Ni(6) atoms], which in turn enhances both the intraplanar bonding between the NN Ni(6) atoms and the interplanar bonding between the NNN Al(1) and Al(2) atoms, and the NNN Ni(3) and Ni(4) atoms. Note that boron also induces an additional charge depletion from all Al atoms. The boron-induced charge density on the (002) plane is shown in Fig. 3(b). Boron induces a substantial enhancement of interstitial bonding charge between the NN Ni(5) sites, increasing thus the intraplanar Ni-Ni bonding within the (002) planes. Finally, an interesting point

Figure 4. Hydrogen-induced charge density of $Ni_3AlH_{\frac{1}{3}}$. Hydrogen occupies the Ni-rich octahedral interstitial site [X(7)]. Solid (dotted) contours represent positive and negative induced charge density. $\pm 8.0 \times 10^{-4}$ e/(a.u.)^3 and increase successively by a factor of $\sqrt{2}$, (a) on the (110) plane (b) on the (002) plane.

to note is that electronic charge is depleted from the interstitial regions near the NiB plane in the [001] direction. This suggests a weaker local cohesion near these planes. This may be due to the fact that the local concentration of boron is high enough in our calculations (7.7 at.%) so as to weaken the local cohesion. This is consistent with the experimental results that Ni_3Al single crystals show a reduced ductility when doped with more than 0.8 at. % boron.[4]

We model the absorbed hydrogen in the supercell geometry of Fig. 1. The hydrogen formation energy is found to be -3.85 eV/(unit cell) and -2.60 eV/(unit cell) for placing the hydrogen impurity at the X(7)(Ni-rich) and X(8) (Ni-deficient) octahedral sites, respectively, indicating that hydrogen also prefers to occupy Ni-rich octahedral sites.

Figs. 4(a) and 4(b) show the impurity-induced charge on the (110) and (002) planes for $Ni_3AlH_{\frac{1}{3}}$. To compare with the boron-induced charge redistribution in Fig. 3(a) and Fig. 3(b), we use the same contour levels for both $Ni_3AlH_{\frac{1}{3}}$ and $Ni_3AlB_{\frac{1}{3}}$. It is clear that hydrogen induces a much weaker charge redistribution than boron. More importantly, the enhancement of interstitial bonding charge found near the pure Ni(6) plane in the [001] direction for the case of boron, is completely missing in the case of hydrogen. Thus, hydrogen does not provide the intraplanar and interplanar bonding enhancement found in the boron doped system. Furthermore, hydrogen affects the more distant nickel atoms [Ni(3)] quite differently. Hydrogen induces a significant build-up of charge along the [001] direction and a charge depletion within the (001) planes containing equal numbers of Ni(3) and Al atoms. This charge redistribution results in an *enhancement* of the *bonding-charge* directionality of Ni(3), which could be interpreted as the signature of a brittle system. Also note that hydrogen causes a larger redistribution of charge on the Ni(3) than on the Al(2) sites, a rather surprising result in view of the larger distance of the Ni(3) atoms from the hydrogen impurity. The

charge redistribution, due to hydrogen, within the (002) plane (Fig. 4(b)) is similar to that induced by boron, which, however, is quantitatively weaker. Overall, while we cannot conclude directly that such a charge redistribution implies brittleness, a comparison of Figures 3(a), 3(b), 4(a), and 4(b) does suggest that hydrogen decreases local crystal cohesion. This is certainly consistent with its role as an embrittling agent.

In conclusion, we have studied the effect of boron and hydrogen on the charge density in Ni_3Al employing first-principles electronic structure calculations based on the FLMTO method. We find that the changes in the electronic structure induced by boron result from the hybridization of the *d* states of the nearest neighbor Ni atoms with adjacent B-*p* states. Thus, boron prefers to occupy Ni-rich octahedral interstices [X(7)]. Boron is found to greatly enhance the intraplanar metallic bonding between the Ni atoms, to enhance the interplanar bonding between the NiAl layers in the [001] direction, and to reduce the bonding-charge directionality near the Ni(3) atoms. Thus, we conclude that in such an environment boron acts to increase the cohesion of the crystal. In contrast, hydrogen is found to enhance the bonding-charge directionality near the Ni(3) atoms and provides virtually no interstitial charge enhancement. This suggests that hydrogen does not promote local cohesion. When both boron and hydrogen are present in the system,[10] the dominant changes in the electronic structure (DOS, induced charge densities) are induced by boron and hydrogen seems to have very little effect.

The research at California State University Northridge (CSUN) was supported through the U.S. Army Research Office under Grant No. DAAH04-93-G-0427, the Lawrence Livermore National Laboratory through Grant No. B157318, and the Office of Research and Sponsored Projects at CSUN. The research at Lawrence Livermore National Laboratory was supported through the U.S. Department of Energy under contract No. W-7405-ENG-48. We have benefited greatly from discussions with Ruqian Wu.

REFERENCES

1. C. T. Liu, in *Alloy Phase Stability*, edited by A. Gonis and G. M. Stocks (Kluwer Publications, 1989), 7.
2. K. Aoki and O. Izumi, J. Jap. Inst. Metals **43**, 1190 (1970).
3. C.T. Liu, C.L. White, C.C. Koch and E.H. Lee, in *High Temperature Materials Chemistry–II* (edited by L.A. Minir and D. Cubicciotti), Vol. **83**, p. 32, Electrochemical Society, Reminton, N.J. (1983); C.L. White, R.A. Padgett, C.T. Liu, and S. M. Yalisove, Scripta Metall. **18**, 1417 (1984); C.T. Liu and C.L. White, Scripta Metall. **35**, 643 (1987); G.S. Painter and F.W. Averil, Phys. Rev. Lett. **58**, 234 (1987); M.E. Eberhart and D. D. Vvedinsky, Phys. Rev. Lett. **58**, 61 (1987);
4. F.E. Heredia and D.P. Pope, Acta Metall. Mater. **39**, 2017 (1991).
5. E. P. George, C. T. Liu, and D. P. Rope, Scripta Metall. et Mater, **27**, 365 (1992).
6. David L. Price and Bernard R. Cooper, Phys. Rev. B **39**, 4945 (1989).
7. N. Masahashi, T. Takasugi, and O. Izumi, Atca Metall. **36** [7], 1815 (1988);
8. D. Hackenbracht and J. Kubler, J. Phys. F **13**, L179 (1983).
9. N. Kioussis, H Watanabe, R. G. Hemker, W. Gourdin, A. Gonis, and P. E. Johnson, Mat. Res. Soc. Symp. Proc. Vol. **319**, 363 (1994).
10. Sheng N. Sun and Nicholas Kioussis, unpublished.

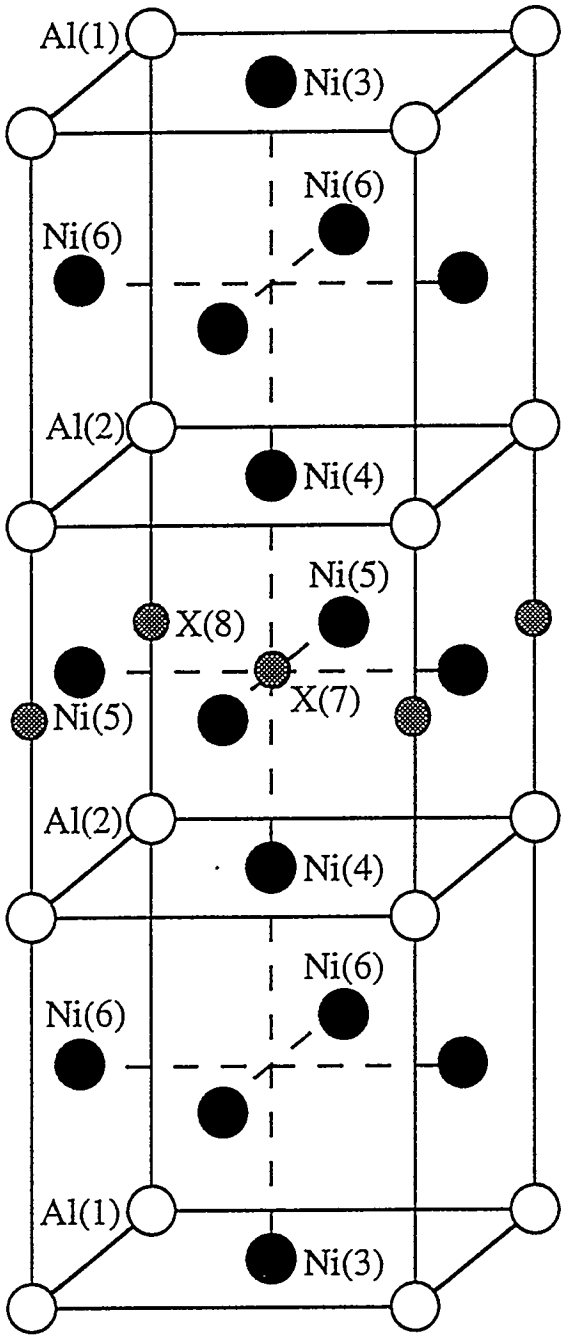

Fig, 1

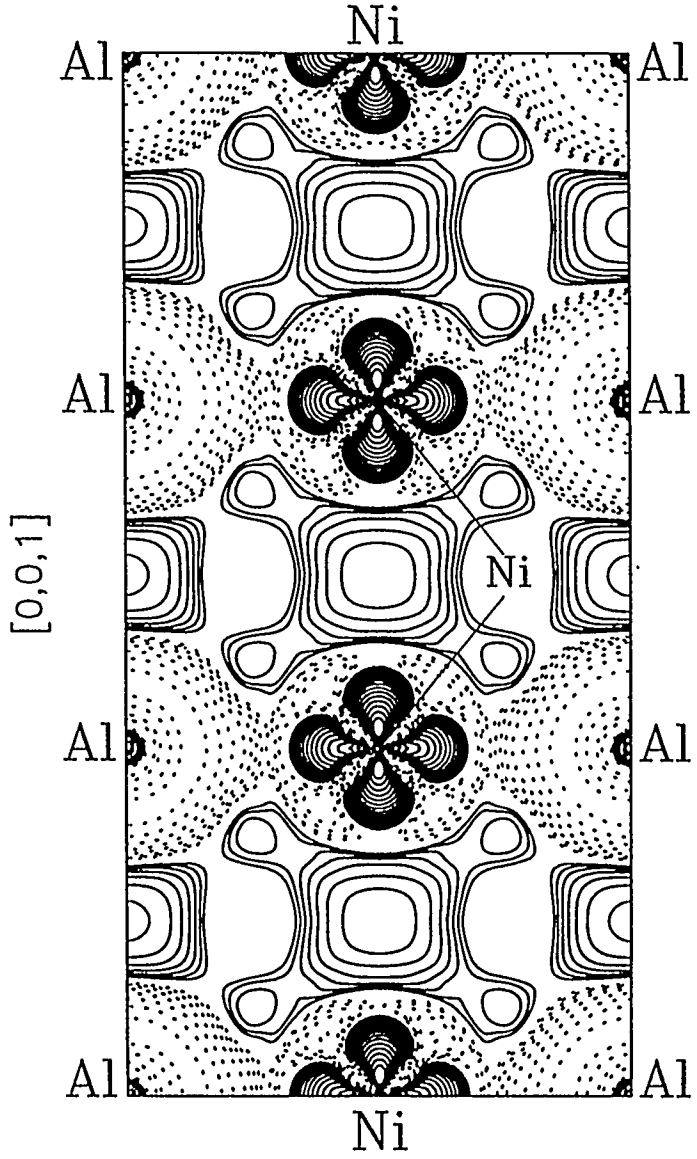

Fig. 2

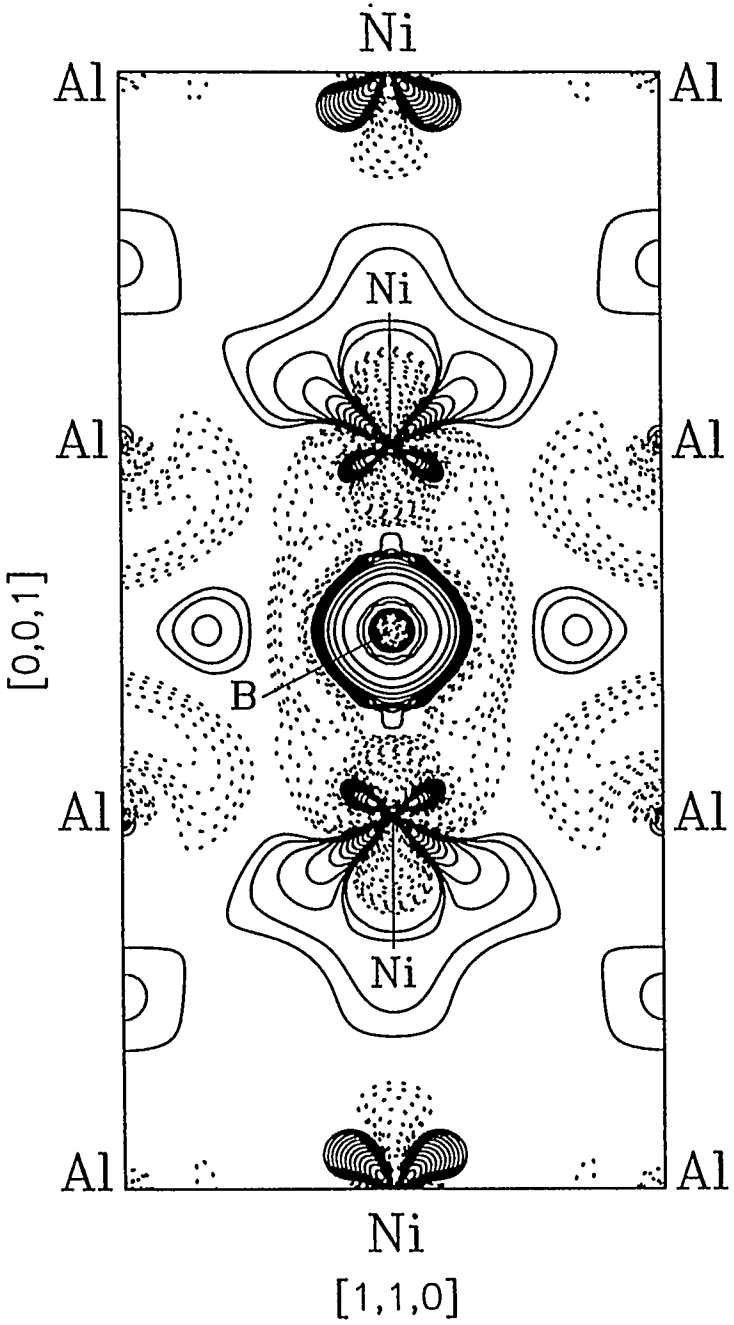

Fig. 3(a)

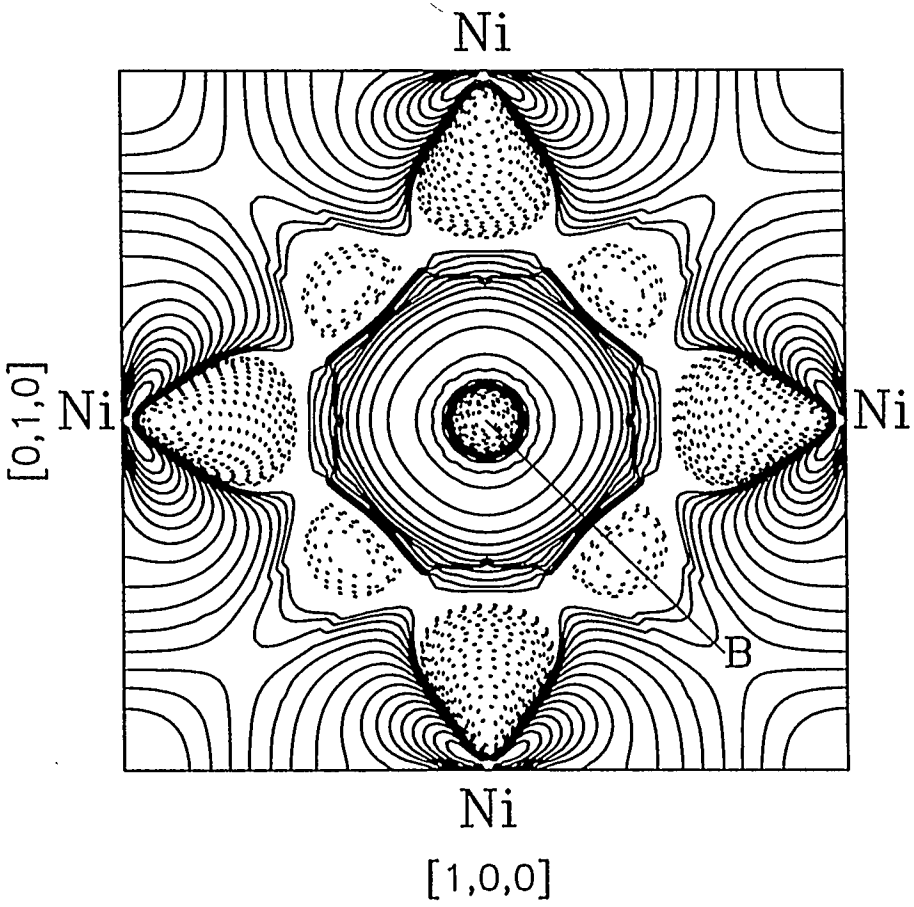

Fig. 3(b)

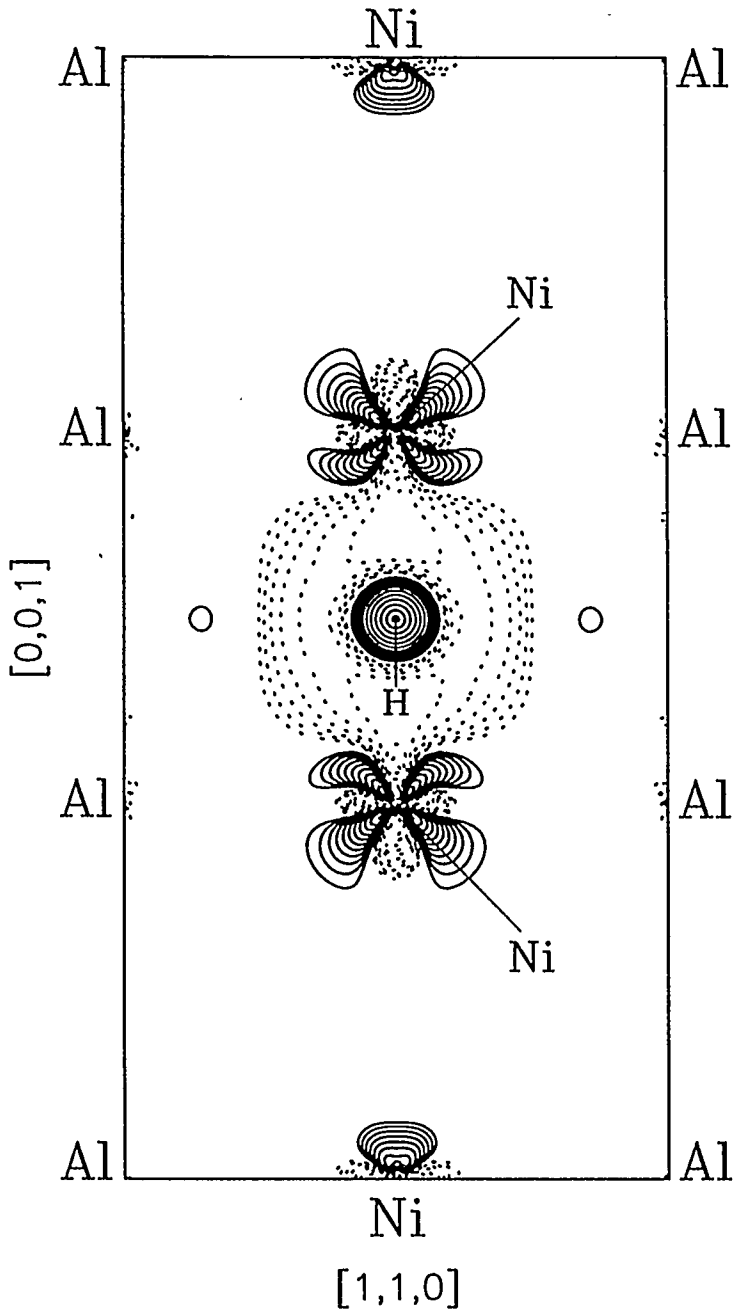

Fig. 4(a)

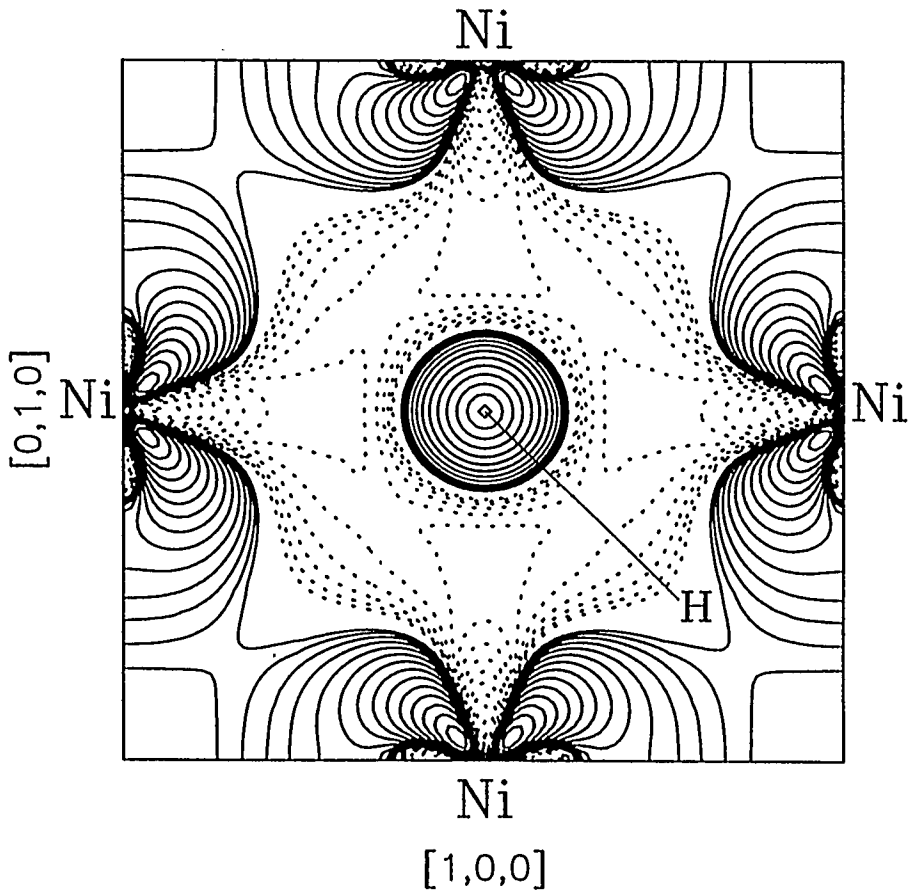

Fig. 4(b)